NASA-CR-201048

6

Report Documentation Page

1. Report No.	2. Government Accession No.	3. Recipient's Catalog No.
SAIC-96/1081 RPT-97-17		

4. Title and Subtitle
A PROOF OF CONCEPT INVESTIGATION: A Unique Mobility Spectrometer for In Situ Diagnostics of Positive and Negative Ion Distributions in the Mesosphere and Lower Ionosphere

5. Report Date
June 17, 1996

6. Performing Organization Code

7. Author(s)
Edward P. Szuszczewicz

8. Performing Organization Report No.

10. Work Unit No.

9. Performing Organization Name and Address
Applied Physics Operation
Science Applications International Corporation
1710 Goodridge Drive
McLean, VA 22102

11. Contract or Grant No.
NASW-4707

13. Type of Report and Period Covered
Final Report

12. Sponsoring Agency Name and Address
Space Physics Division
National Aeronautic and Space Administration
Washington, DC 20546

14. Sponsoring Agency Code

15. Supplementary Notes

16. Abstract We have carried out a proof-of-concept development and test effort that not only promises the reduction of parasitic effects of surface contamination (therefore increasing the integrity of "in situ" measurements in the 60-130 km regime), but promises a uniquely expanded measurement set that includes electron densities, plasma conductivities, charged-particle mobilities, and mass discrimination of positive and negative ion distributions throughout the continuum to free-molecular-flow regimes. Three different sensor configurations were designed, built and tested, along with specialized driving voltage, electrometer and channeltron control electronics. The individual systems were tested in a variety of simulated space environments ranging from pressures near the continuum limit of 100 mTorr to the collisionless regime at 10^{-6} Torr. Swept modes were initially employed to better understand ion optics and ion "beam" losses to end walls and to control electrodes. This swept mode also helped better understand and mitigate the influences of secondary electrons on the overall performance of the PIMS design concept. Final results demonstrated the utility of the concept in dominant single-ion plasma environments. Accumulated information, including theoretical concepts and laboratory data, suggest that multi-ion diagnostics are fully within the instrument capabilities and that cold plasma tests with minimized pre-aperture sheath acceleration are the key ingredients to multi-ion success.

17. Key Words (Suggested by Author(s))	18. Distribution Statement
"In Situ" Measurement Techniques, Mesosphere, Thermosphere, Ionosphere	

19. Security Classif. (of this report)	20. Security Classif. (of this page)	21. No. of pages	22. Price
Unclassified	Unclassified	29	

NASA FORM 1626 OCT 86

Table of Contents

1. EXECUTIVE SUMMARY

We have carried out a proof-of-concept development and test effort that not only promises the reduction of parasitic effects of surface contamination (therefore increasing the integrity of *in situ* measurements in the 60 -130 km regime), but promises a uniquely expanded measurement set that includes electron densities, plasma conductivities, charged-particle mobilities, and mass discrimination of positive and negative ion distributions throughout the continuum to free-molecular-flow regimes.

The instrument concept under test in this investigation has a configuration that resembles a retarding potential analyzer. But its operation is significantly different. Using pulsed-voltage time-of-flight techniques, we call the new instrument concept a pulsed ion mobility spectrometer (PIMS).

Three different sensor configurations were designed, built and tested, along with specialized driving voltage, electrometer and channeltron control electronics. The individual systems were tested in a variety of simulated space environments ranging from pressures near the continuum limit of 100 mTorr to the collisionless regime at 10^{-6} Torr. Quasi-Dc (i.e., swept) modes were employed in the early stages to better understand ion optics and ion "beam" losses to end walls and to the discriminator and suppresser electrodes. This swept mode also helped better understand and mitigate the influences of secondary electrons on the overall performance of the PIMS design concept.

Final results demonstrated the utility of the concept in dominant single-ion plasma environments but precise multi-ion diagnostics were illusive because of temperature spreading in the ion distributions created in the laboratory plasma. Accumulated information, however, including theoretical concepts and laboratory data, suggest that multi-ion diagnostics are fully within the instrument capabilities and that cold plasma tests with minimized pre-aperture sheath acceleration are the key ingredients to multi-ion success. These improvements are discussed along with the "lessons learned' in the PIMS proof-of-concept effort.

2. BACKGROUND AND RELEVANCE TO NASA OBJECTIVES

2.1 Overarching Science Requirements

In recent years the Space Physics Division has expanded its charter to include the thermosphere and the mesosphere, with a thrust that focuses on the coupling processes that integrate the ionospheric-thermospheric-mesospheric (ITM) system as a whole.[1,2] This proof-of-concept activity responds to that new thrust with attention to the diagnostic problems associated with charged-particle measurements in the altitude region from 60-130 km. This altitude encompasses the mesosphere and the lower regions of the ionosphere and thermosphere. It is

for important applications to this unique regime that we proposed to develop a unique experimental tool that will accurately determine charged-particle distributions over the full altitude extent and establish the fundamental role of these distributions in the Earth's electrodynamic circuit.

Our focus involved the most complex naturally occurring plasma domain accessible to *in situ* and remote-sensing measurement techniques. This is a region with processes in the continuum, transitional, and free-molecular flow regimes. It is dynamically responsive to kinetic and electrodynamic forces, and it involves positive and negative ion chemistry with clustered-ion masses in excess of 100 amu.

In regions where collision kinetics provide the dominant force (Z < 75 km), the conductivity is a scalar and the electric fields and currents are parallel. At higher altitudes, the electrons become decoupled from the atmospheric constituents and are controlled more by the ambient magnetic field. Under these circumstances, the conductivity becomes a tensor; and the electric fields and current systems are no longer parallel. This transition from a scalar to a tensor conductivity also marks the transition from continuum to free-molecular flow and defines our altitude of interest, 60-130 km. This change in conductivity also includes dramatic changes in ion composition and impacts the mapping of ionospheric and magnetospheric electric fields downward into and through the middle atmosphere.

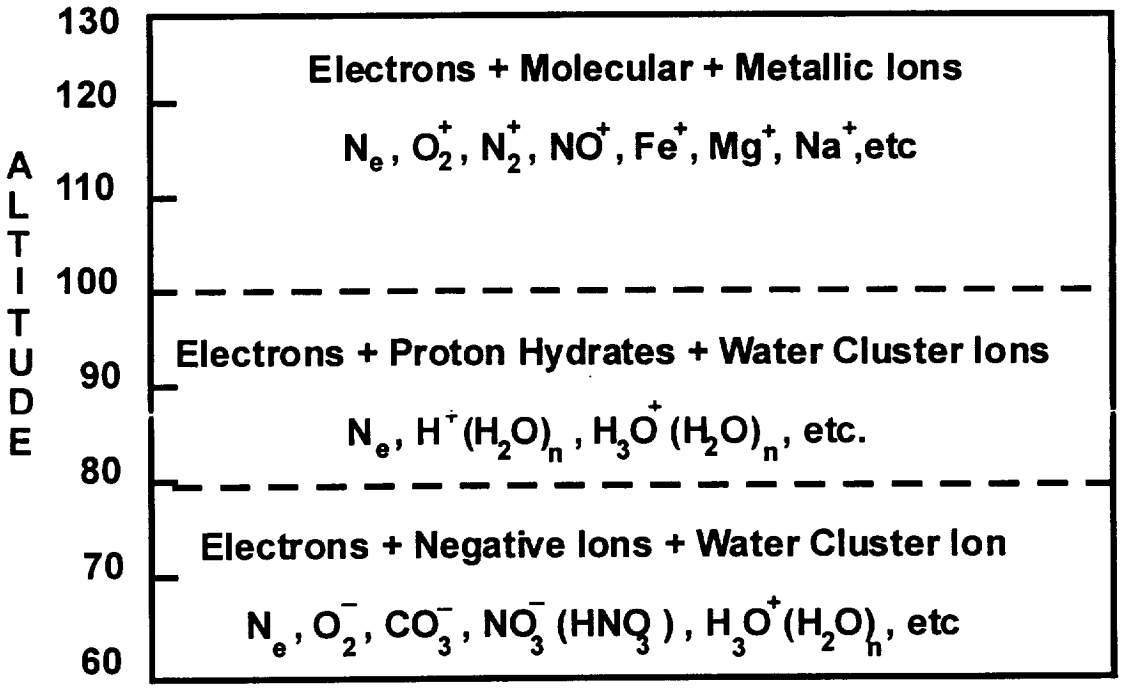

Figure 1. Approximate Regions of Unique Charged-Particle Composition in the Lower/Thermosphere-Ionosphere and Mesosphere.

The ion distributions have three unique altitude regimes[3-5] as illustrated in Figure 1. At altitudes between 100 and 130 km, the charged particle population is dominated by free electrons and positive ions, including the moleculars N_2^+,O_2^+, and NO^+, and several metallics (e.g., Fe^+, Mg^+, Na^+). Below 100 km, there is a sharp transition in the positive ion composition to proton hydrates (i.e., $H^+(H_2O)_n$) and water-cluster ions (i.e., $H_3O^+(H_2O)_n$). At yet lower altitudes (<80km), negative ions begin to play a significant role. Free electrons can become non-existent and the negative ion population can define the entire negative charge distribution.

> According to the ITM panel report[2] for the Strategy Implementation Study, *"The distribution of charged particles within the mesosphere remains as one of the outstanding questions of the ITM system. While it is generally agreed that the mesosphere is populated with free electrons and positive and negative cluster ions, reliable measurements and associated theoretical models are non-existent. This lack of information exacerbates the related controversy involving mesospheric electric fields, known to span seven orders of magnitude, with speculation that causal mechanisms are attributable to the existence of charged aerosols. These issues are fundamental to the understanding of mesospheric electric field distributions current systems, overall considerations of conductivity, and electrodynamic coupling to the ionosphere."*

2.2 Diagnostic Problems

The complexity of this lower ITM environment has its counterpart in problems which plague the *in situ* diagnostic techniques that have been applied to its investigation. Generally accessible only to rocketborne payloads, difficulties have revolved around the breakup of ion clusters or the detachment of electrons from negative ions by shocks and large draw-in potentials,[6,7] and the problem of contamination, known for years to degrade *in situ* plasma diagnostic techniques,[8] can have serious parasitic effects on the measurements in the high-pressure, water-cluster-ion environment of the mesosphere.

For the regions below the mesopause (~100 km), measurement techniques have focused on bulk electrical properties,[9] such as mobility, conductivity, and ion density. Direct applications of ion mass spectrometry have also been used for determination of the ion composition, with some of the more serious problems having arisen in the measurement of negative ions.[3,4] More simple Langmuir-type two-electrode techniques like the blunt probe and the Gerdien condenser are used more frequently. The blunt probe uses a planar disc with a concentric guard electrode, while the Gerdien employs a cylindrical-capacitor double-electrode design. Both are electrically operated much like conventional

Langmuir probes, with a slowly varying potential yielding a current-voltage characteristic that is linearly dependent on the conductivity.

The Gerdien condenser has had wide application in measurements of ion mobility, conductivity, and ion concentrations. The results, however, seem to be mixed. While Mitchell[9] reports favorable comparisons, there remains a plaguing set of inconsistencies. In rocketborne applications, there seems to be no general agreement among the various measurements,[6] with the suggestion that the Gerdien measurements may have been affected by the breakup of cluster ions by both shock waves and instrumental electric field effects. The inconsistencies also appear to develop in the Gerdien's determination of ion concentration, where again there have been puzzling differences between observations and predictions.[6]

Inconsistencies and conflicts in mesospheric measurements include not just ion composition, conductivity, and mobility; but they include electric fields as well. Most controversial of all have been observations of electric field strengths that are an order of magnitude larger than those required to maintain the fair-weather current.[3,10,11] The quality of these measurements has been questioned; and the possibility of instrumental effects is still an open issue.[12]

All the instruments we have discussed contain a common feature. They are all effectively dc or slowly swept devices that demand stable sensor-electrode potentials for the integrity of the measurement. The mass spectrometer has an aperture plate with an ion-attracting potential that, in effect, establishes it as a planar fixed-bias blunt probe. Electric field devices are also Langmuir probes held at the local floating potential by high-impedance amplifiers; and the Gerdien is similar to a double probe with asymmetric geometries in the two-electrode system.

These dc and quasi-dc measurements are susceptible to large errors in the high-pressure, collision-dominated mesosphere. Our experience shows that surface potentials can vary radically during a measurement period and may severely distort the measurement results[13,14] in laboratory plasmas, in contaminating environments around rocket and shuttle payloads, in environments at high pressures, and in gaseous mixtures involving water molecules.

Clearly, there is need for a new approach, an approach that is different from the quasi-dc techniques that have been employed to date. There is also a need to develop an approach that can measure electron and positive/negative ion concentrations with an intrinsic mass discrimination capability. There is the need to develop a technique that can cover the entire altitude region from 60-130 km in order to diagnose the transitions from scalar-to-tensor conductivities, from continuum-to-collisionless behavior, and from negative/positive cluster-ion plasmas to "conventional" electron/positive-ion plasma environments. There is also the need to understand the fate of metallic ions that are routinely brought into the mesosphere from the lower ionospheric-thermospheric domain by

intermediate and descending layers.[15,16] Are the descending layers of metallic ions in the lower ionosphere (100-150 km) the primary source of the intense Na and Fe layers observed by lidar[19,20] in the 80-95 km domain? And is there any sense in the speculation that the metallic ions are somehow recycled in the upper mesosphere to the equatorial region and transported back into the ionosphere by the fountain effect?[17,18]

There is little question that there is a genuine need for a new, more accurate, and more comprehensive diagnostic approach in order to achieve an integrated perspective on the electrical properties in the lower ionospheric-thermospheric-mesospheric system and the coupling mechanisms that bind them as a single unit.

3. THE APPROACH

3.1 The Sensor Concept

We undertook a proof-of-concept development effort that not only reduced the parasitic effects of surface contamination therefore increasing the integrity of *in situ* measurements in the 60-130 km regime, but promises a uniquely expanded measurement set that will include electron densities, plasma conductivities, charged-particle mobilities, and mass discrimination of positive and negative ion distributions throughout the continuum to free-molecular-flow regimes.

Illustrated in Figure 2, the concept has an instrument configuration that resembles a retarding potential analyzer.[21] But its operation is significantly different. Using pulsed-voltage time-of-flight techniques, we call the new instrument concept a pulsed ion mobility spectrometer (PIMS) with components that include:

1. An *aperture* in direct contact with the ambient plasma. The aperture is composed of an outermost guard ring electrode with an inner concentric ring called the *aperture probe.* The aperture probe has as its center a wire mesh opening to allow passage of ambient species into the time-of-flight mass discrimination region of the device;

2. A *discriminator electrode* to control the charged species entering the main body of the detector;

3. A *suppresser* to reflect secondary electrons that may be emitted from the collector; and

4. A guarded *collector* with a pinhole opening for *channeltron* sampling.

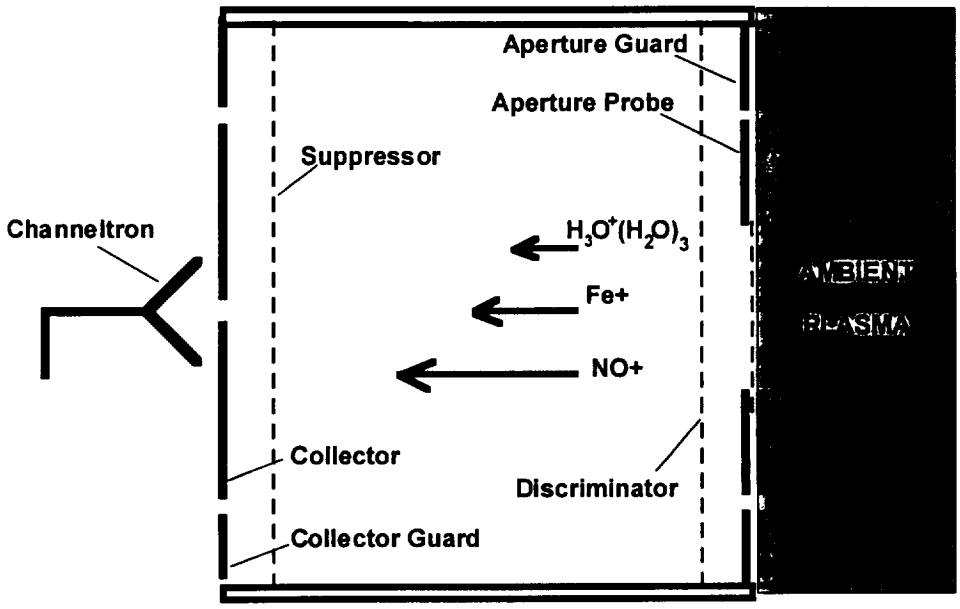

Schematic Illustration of Mobility Spectrometer

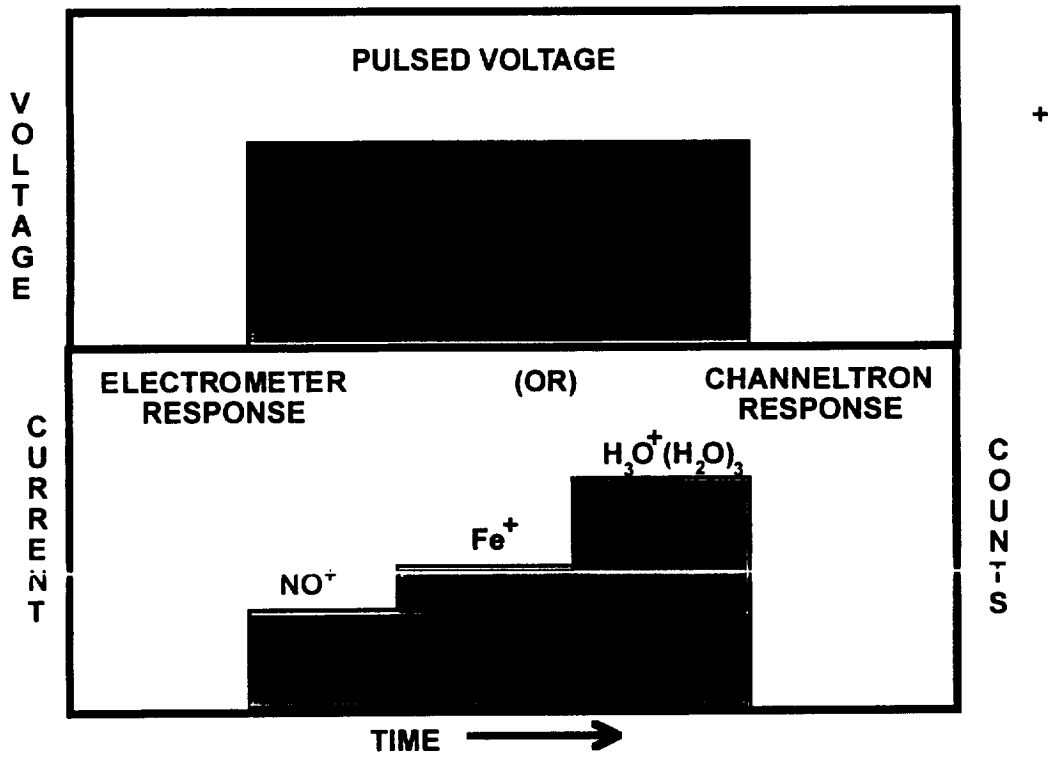

Illustration of Electrometer (or Channeltron) Response in a Three Ion Plasma

Figure 2. The PIMS instrument concept (top panel) and time-dependent mass-sensitive pulsed-voltage current responses to a positive ion plasma with three ion components (bottom panel).

In the operational concept, the aperture has an applied potential that is near the local plasma potential, so that there is little-to-no sheath external to the device and only non-accelerated thermal particles can enter the detector. In positive-ion mode, the discriminator is biased positively relative to the aperture, effectively defining the positive ion boundary at the aperture; and the collector and suppresser are biased negatively with respect to the discriminator (e.g., by 2-10 volts) in order to repel electrons, and set up a field to attract positive ions to the collector and channeltron sampling regimes.

At a time T_0, a fast-rising negative pulse (approximately two volts negative with respect to the ambient plasma potential) is applied simultaneously to the discriminator and the collector-suppresser system. This allows positive ions, previously repelled by the discriminator, to enter the device and be attracted to the collector by the discriminator bias voltages. The positive ions then arrive at the collector with temporal characteristics that represent the mass and density distributions of the ions in the ambient plasma and the level of collisionality with the ambient neutral species. Figure 3 plots the ideal time-of-flight histories for ions between mass 16 and 100 amu, assuming detector lengths L of 2 and 10 cm and attracting potentials V (between the collector and discriminator) of 2 and 10 volts. The top and bottom panels in Figure 3 reflect free-molecular and continuum-flow conditions, respectively. This is equivalent to the conditions at 130 km and 60 km, respectively.

Focusing on the collision-free case with (L,V) = (2cm, 2v), we can see that NO^+ will arrive at the collector in approximately 10 μs, while the water cluster ion $H_3O^+(H_2O)_3$ arrives 5μs later. In the collisional case, the times would be 0.23 ms and 0.7 ms, respectively. If yet a third ion (e.g. Fe^+) were involved, its arrival time would fall between the first two species, with the resulting three-ion-plasma electrometer response ideally illustrated in the lowest panel in Figure 3. Under these circumstances, the device could discriminate ion masses and determine densities through measured fluxes and known accelerated velocities.

3.2 Supporting Concepts, Instrumentation, and Design Technology

The PIMS concept is a natural extension of several successful new instrument design concepts and it draws on accumulated experience in laboratory, rocket-, satellite-, and parachute-borne plasma diagnostic techniques covering altitude ranges from 40 km to the topside ionosphere. These technologies and experimental learning experiences are reflected in the conceptual design, with relevant issues discussed in the following sections.

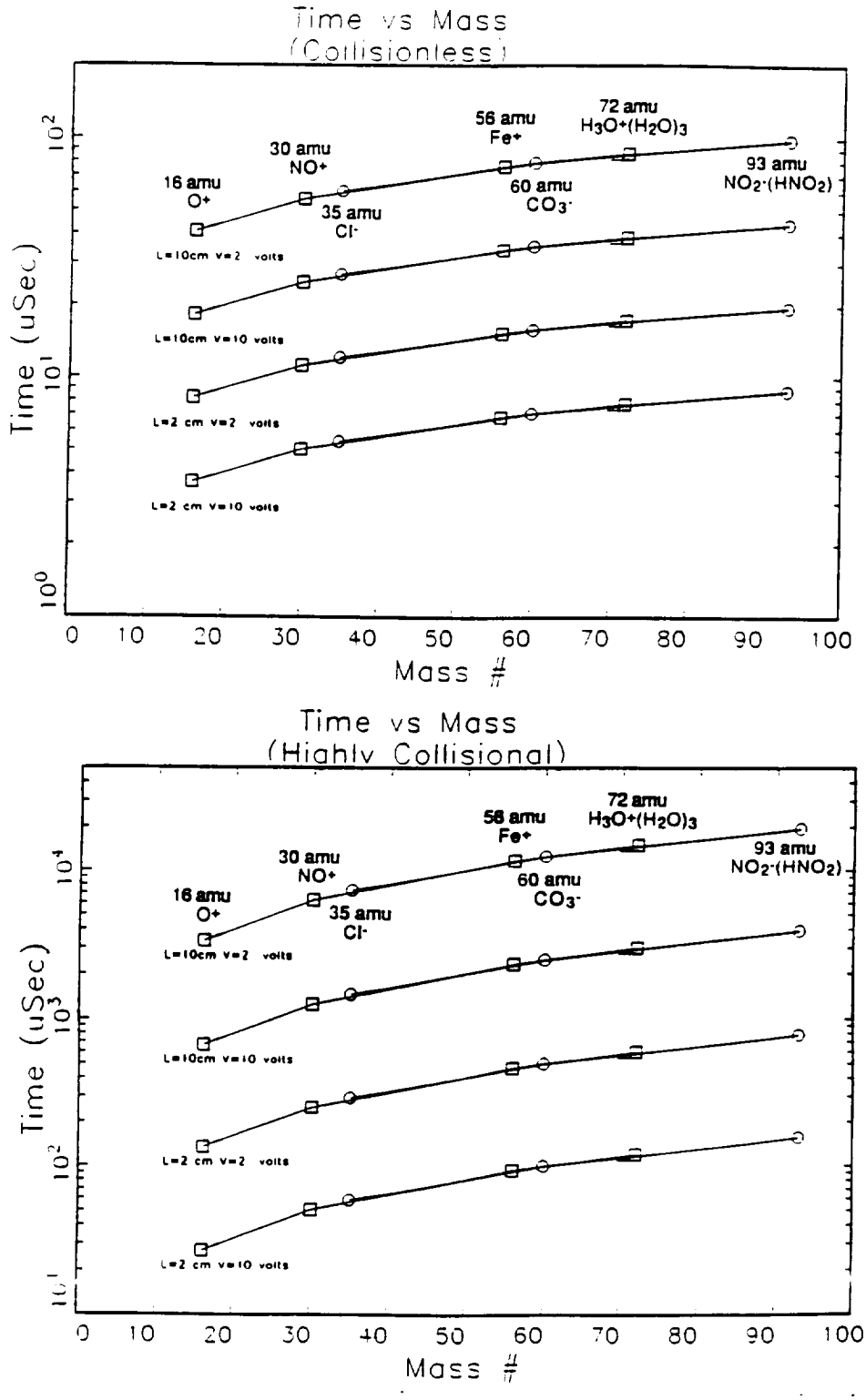

Figure 3. Time-of-flight simulation results for positive and negative ions in a PIMS detector with a time-of-flight length L (distance from the discriminator to the collector) taken at 2 and 10 cm and an absolute voltage differential of 2 and 10 volts. The upper panel corresponds to the collision-free case and an approximate altitude of 130 km. The bottom case corresponds to a highly collisional continuum case and an approximate altitude of 60 km.

3.2.1 Contamination Effects and Measurement Reliability

Laboratory investigators and space plasma experimentalists have known that electrode containment can result in serious degradation of any measurement technique that requires stable potentials for the integrity of the measurement. This applies to mass spectrometer apertures, blunt probes, Gerdien condensers, electric field detectors, and Langmuir probes. In each instance, the electrode operates as one form of Langmuir probe, so that probe problems with contamination reflect a generic problem area for all such instruments.

With regard to conventional fixed-bias and continuous-sweep approaches to Langmuir probe (blunt probe and Gerdien) diagnostics, studies have shown that contaminating environments can seriously compromise the measurement results through temporal variations in the surface work function.[22-26] A telltale manifestation of surface contamination is hysteresis in the *I-V* characteristic, whereby the *I-V* response is not identically reproduced in the positively and negatively sloped portions of the applied probe voltage (up and down arrows in the top panel of Figure 4). This behavior is attributed to the time-, voltage-, and current-dependent layering of foreign material on the surface of the probe, resulting in a variation of the work function, distortion of all gradients in the characteristic, and degradation of inferred plasma parameters.

A model[23] for the surface-layering phenomenon is illustrated in the top panel of Figure 4, which schematically depicts a contaminated probe in a plasma. The mechanisms for the development of the surface layer of contamination are not always easily identified, but contributions may come from the deposition of sputtered material from other solids in the system or from the sorption of gases and vapors in the plasma. (Water and oil vapors are especially problematic, even at extremely trace levels.) A perfectly cleaned and outgassed probe, when immersed in any medium, immediately absorbs and occludes the ambient species.[25] If these species are nonconductive, or are composed of polar molecules, a capacitively coupled insulating layer will develop. This layer is modeled by the capacitance C_c and leakage resistance R_c in Figure 4. When a plasma is part of the environment and a voltage V is applied to the probe, charged particles will flow to the probe's contaminated surface, charge up the associated capacitance C_c, and simultaneously alter the absorbate surface layer by bombardment.[26] These conditions and their associated dependence upon the applied probe voltage bring about the hysteresis in the current-voltage characteristic. It is possible to sweep the probe voltage so slowly that the (I,V) data points come to identical equilibrium values in the up and down legs of the sweep.[23] In this case, the measurements are still in error; but the investigator does not have the advantage of telltale hysteresis.

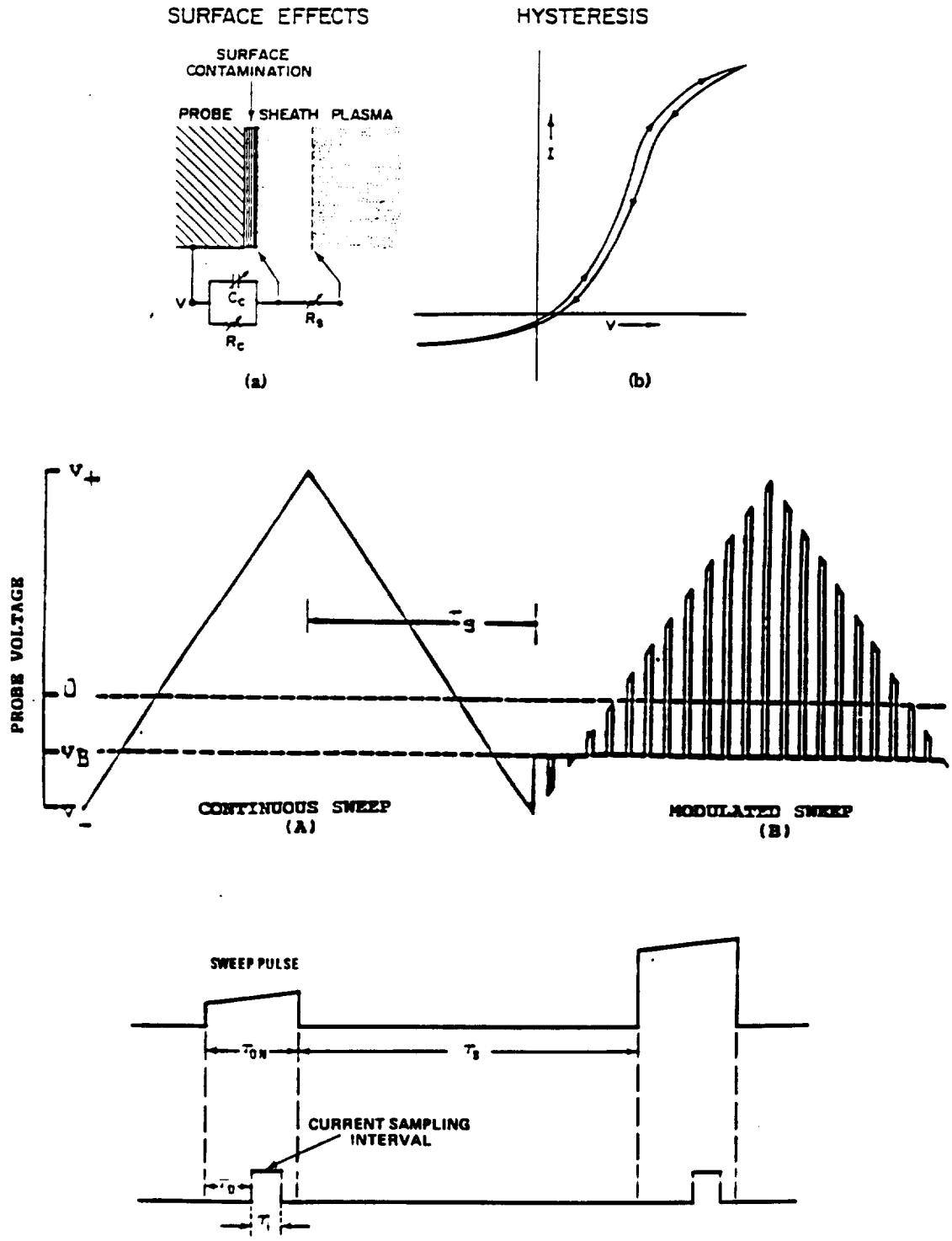

Figure 4. Top panel: Phenomenological circuit model for surface contamination on an electrode immersed in a plasma with a telltale hysteresis effect in the I-V characteristic. Middle panel: Illustration of voltage formats applied in conventional approaches to Langmuir probes (left side compared with the approach of the pulsed-plasma-probe, P^3 (right side). Bottom panel: Expanded view of the P^3 voltage pulsing sequence showing the sweep pulse and baseline periods.

When surface contamination is a problem, conventional Langmuir-type probe measurements have distorted slopes in the retarding-field and saturation-current regions, with associated measurement errors in the densities and temperatures. As indicated in the top panel of Figure 4, contamination can also result in an unknown offset voltage V_c across the layer, contributing to uncertainties in determining the actual voltage imposed on a plasma by fixed-potential electrodes. *These problems may be resolved by eliminating the contaminating species from the system or modifying the experimental technique. The former approach is not always feasible, making it incumbent upon the experimenter to modify his technique so that it is not susceptible to distortion by contamination.*

To eliminate the aforementioned problems and to improve the reliability and versatility of Langmuir-type probe measurements, a pulsed plasma probe (P^3) technique[8,22] has been developed. The approach employs a pulsed-voltage procedure designed to maintain a constant surface condition throughout the collection period of the I-V characteristic; that is, the technique allows the existence of a contamination layer but keeps the layer and its associated potential drop at a constant level. The middle panel of Figure 4 depicts two voltage sweep modes for Langmuir probe operation. The left side of the panel shows a continuous sweep voltage which represents the conventional approach to Langmuir probe (Gerdien condenser and blunt probe) measurements, while the right side shows the waveform used in the P^3 technique. The P^3 approach employs a series of voltage pulses (~100μs wide) which follow a sawtooth envelope. During the interpulse period (~900μs), the probe is held at a fixed baseline voltage level V_B which is generally positioned in the ion or electron saturation region of the probe's I-V characteristic. The long (relative to the 100 μs pulse) baseline voltage level stabilizes surface conditions between pulses (reducing hysteresis effects and erroneous measurements of temperature and density); and running measurements of baseline currents provide a measure of plasma density variations, density fluctuation power spectra, and associated turbulence structure.[27,28] The continuous measurement of baseline current also allows the unfolding of a Langmuir I-V characteristic when density variations occur on a time scale short compared to the probe's sweep period.[28]

The P^3 technique, in its successful treatment of the contamination problem and diagnostics of dynamic plasma environments, has been applied in a wide variety of laboratory and space plasma investigations. Its history includes over 14 rocket investigations, the S3-4 Ionospheric Irregularities Satellite Mission, the first DoD Shuttle flight, detailed laboratory studies of energetic particle beam interactions with plasmas, and CRRES satellite studies of chemical releases in space.

3.2.2 The PIMS Pulsed Voltage Approach to Retarding Potential Analysis

The Plasma Potential and Particle Distribution and Density Detector $(PD)^3$ was developed at SAIC to combine the capabilities of the pulsed-plasmas-probe (P^3) technique (discussed in the previous section) with the concept of a directional retarding potential analyzer (RPA), capable of modest pitch-angle resolution and fast-response energy measurements under dynamically variable plasma conditions. The $(PD)^3$ measures the thermal and suprathermal energy distributions of incident ions and electrons, while simultaneously determining the electron density, density fluctuation power spectra, temperature, and local plasma potential. These capabilities are realized using a modified RPA geometry, with interleaving pulsed-voltage formats on the aperture and discriminator grids.

The top panel in Figure 5 shows a cross section of the PD^3 detector, and reveals its internal grid structure. The device has a micro-channel aperture plate with a concentric guard electrode, two internal grids for the particle discrimination and secondary electron suppression, and a collector surface at which currents are measured. The geometry of the micro-channel plate gives the instrument a 45° field-of-view and ensures that about 50% of the incident particles are collected on the aperture. The portion of the incident particles which pass through the aperture are energy analyzed within the device, using the scheme described below.

The bottom panel of Figure 5 shows an example of the pulse sequences applied to the various $(PD)^3$ surfaces. The aperture has two baselines, one at +3 volts for electron and negative ion measurements, and one at -3 volts for the measurement of positive ions. Pulses to the aperture trace a triangular wave envelope, which results in the measurement of a P^3-type I-V characteristic on the aperture. The plasma density, temperature and potential are derived from these I-V characteristics, just as they are for the P^3 technique discussed in the previous section.

During the inter-pulse period on the aperture (typically 1.6 ms) a fixed baseline voltage is maintained. When the baseline voltage is +3 volts, electrons and negative ions are drawn toward the aperture, and when the baseline is negatively biased, positive ions are drawn in. Some of these incident particles pass through the aperture and enter the energy analysis region of the $(PD)^3$. These baseline voltage levels not only allow entrance of selected charged species into the detector but the associated baseline current measurements track ambient density fluctuations which can be unfolded from the aperture's I-V characteristic and from the flux-dependent energy analysis of the $(PD)^3$ collector currents.

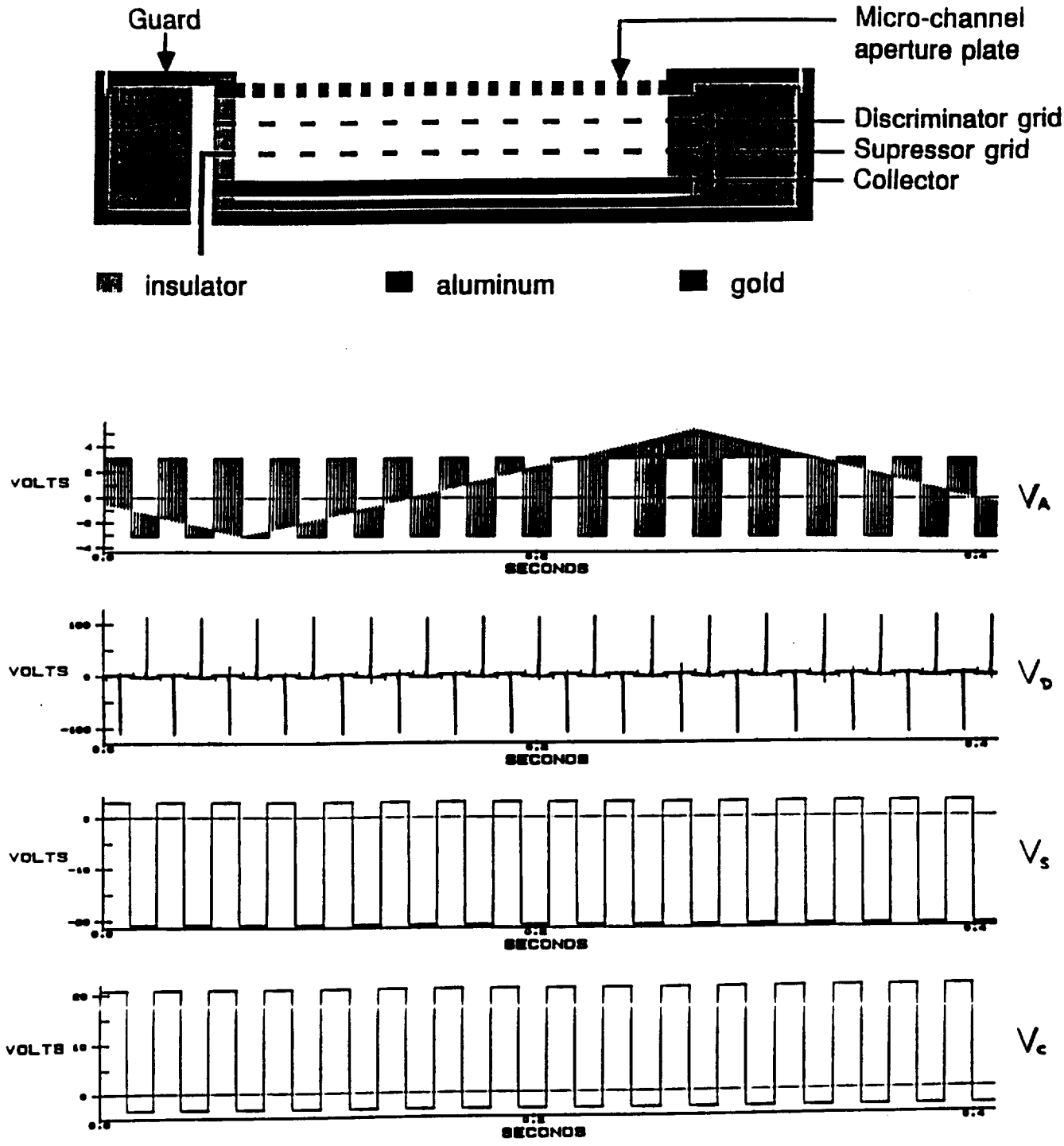

Figure 5. Top panel: Illustration of the (PD)^3 device. Bottom panel: Voltage-pulsing sequence applied to the anode V_A, the discriminator V_D, the suppresser V_S, and the collector V_C. An expanded view of V_D is shown in Figure 6.

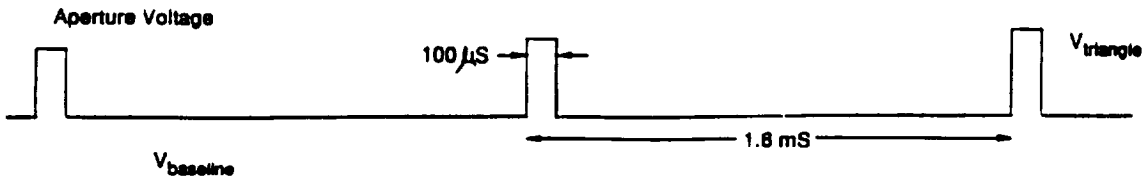

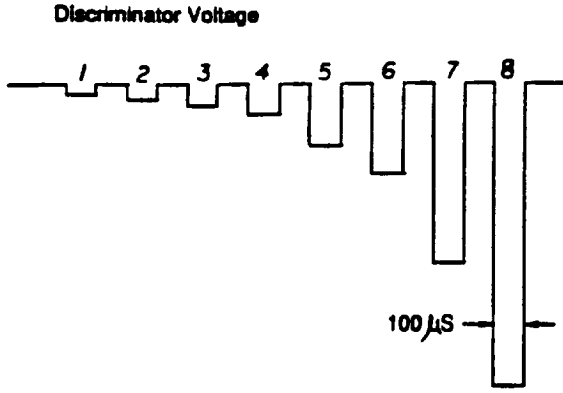

	Pulse Number							
Mode	1	2	3	4	5	6	7	8
Thermal Ion	0.2	0.3	0.6	1.0	2.0	3.0	6.0	10.0
Energetic Ion	2.0	3.0	6.0	10.	20.	30.	60.	100.
Thermal Electron	-0.2	-0.3	-0.6	-1.0	-2.0	-3.0	-6.0	-10.0
Energetic Electron	-2.0	-3.0	-6.0	-10.	-20.	-30.	-60.	-100.

I_A monitored at 800 μS intervals

I_C monitored during discriminator pulses, read out from 5 & 7 over 0.4 mS

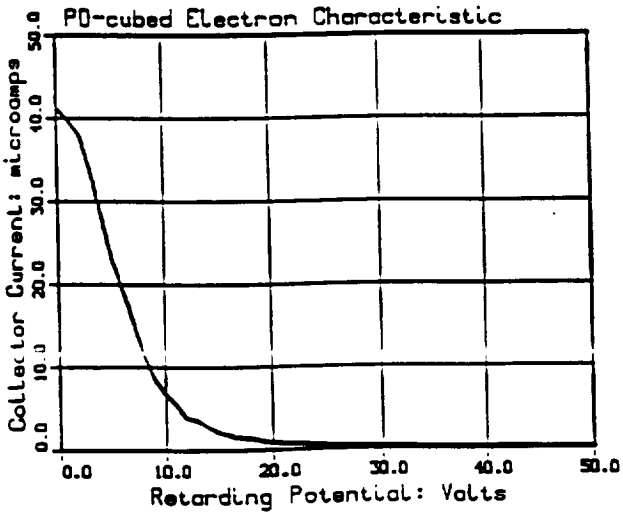

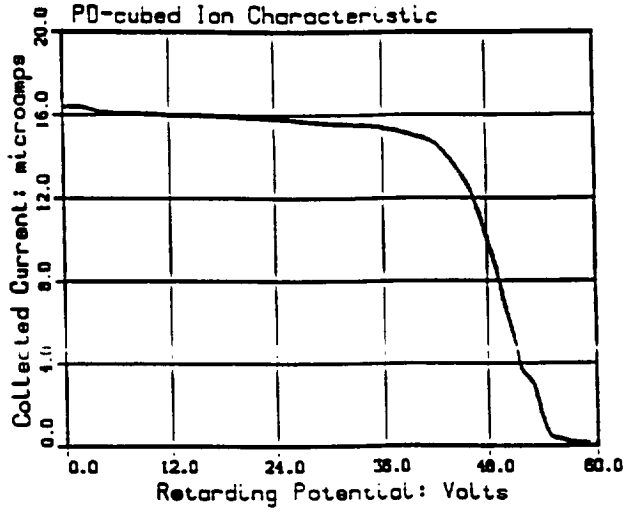

Figure 6. Top panel: An expanded view of the discriminator voltage-pulsing sequence during the baseline period of the anode potential. Bottom panel: $(PD)^3$ electron and ion I-V characteristics on the left and right sides, respectively. Conditions include an argon plasma at 2.5 m Torr with 25 watts of power applied to the inductively coupled hf discharge.

After passing through the aperture, incident particles encounter the discriminator grid. The potential of this grid is biased with a voltage-stepping series of 100μ pulses applied at a 5 kHz rate, as shown in the top panel of Figure 6. In this mode, an RPA- type I-V curve can be generated (in this case with course energy resolution) in 1.6 ms. The magnitude of the collector current is proportional to the density of collected particles (those having energies greater than the discriminator voltage), so the energy distribution can be derived from the collector current characteristics.

The basic collector measurement yields a curve showing the collector current as a function of discriminator voltage, as shown in the laboratory test results in the bottom panel of Figure 6. The curves represent the ion and electron fluxes to the collector as the discriminator's retarding voltage is varied. When the retarding voltage is small, nearly all of the particle population that passes through the aperture is collected. As the retarding voltage on the discriminator increases, the lower energy particles are repelled and the collector current decreases. In multicomponent plasmas, the characteristic curves are more complex. In these cases, curve fitting routines are used to identify the component ion populations and estimate their densities, assuming the distributions are Maxwellian.

In summary, the $(PD)^3$ technique combines the measurement capabilities of a planar P^3 and a fast-response directional RPA into a single instrument. By a proper interleaving of the pulse sequences on the various grids and surfaces, it is possible to provide highly time-resolved measurements of the plasma density, potential, electron temperature, and thermal and suprathermal ion energy distributions simultaneously. This is done with minimum concern about surface contamination and with the capability to unfold density fluctuations from the aperture's (P^3-like) I-V characteristic and collector current characteristics used for ion energy determination. This technique is applicable in both laboratory and spacecraft environments and uses existing microprocessor-based control and electrometer circuitry.

4. IMPLEMENTATION AND RESULTS

4.1 Laboratory Facilities for Proof-of-Concept Testing

Our approach to the development and test of the PIMS concept included hands-on instrument development experience and unique space plasma test and simulation facilities. Within our laboratory we operate two simulation chambers illustrated in Figure 7.

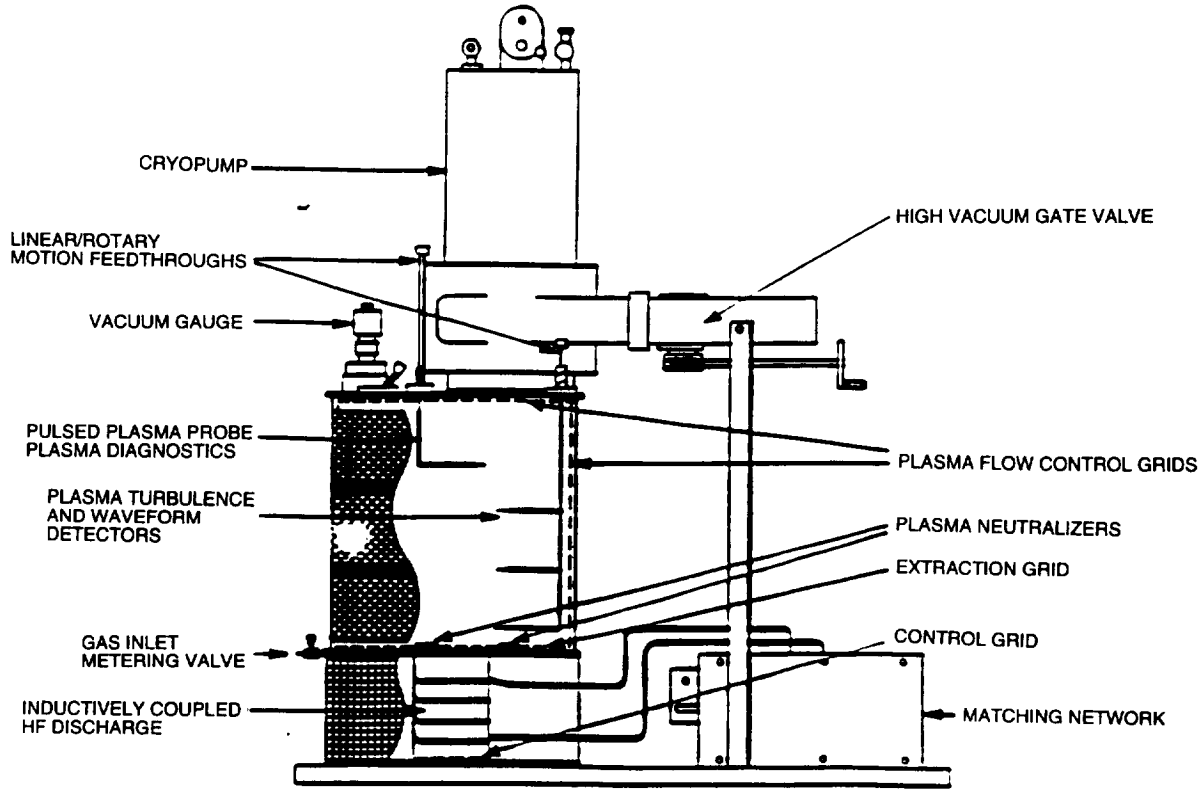

Chamber A

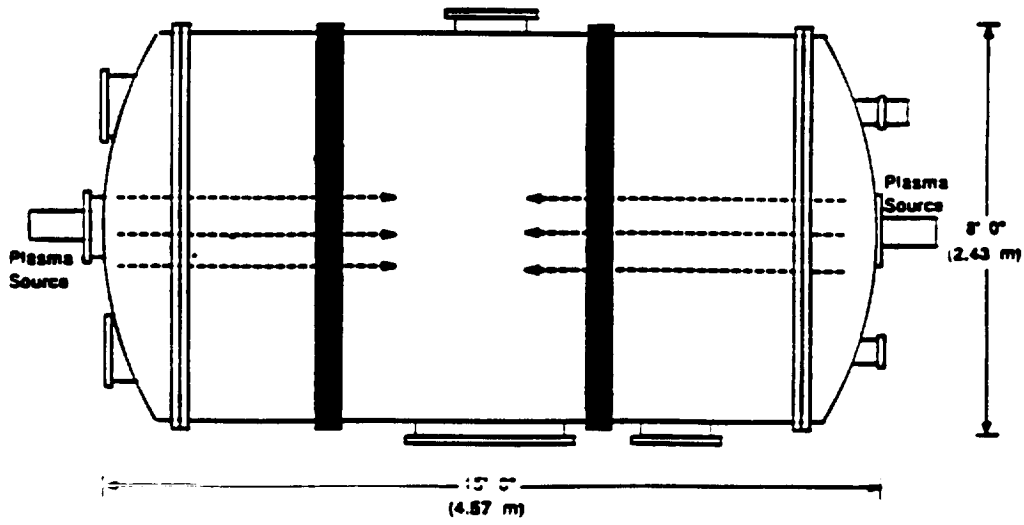

Chamber B

Figure 7. Space plasma simulation and test facilities within SAIC's Laboratory for Atmospheric and Space Sciences. Unique components include large chamber size and plasma sources that can simulate the positive and negative ion distributions in the lower ionosphere and the mesosphere. The large chamber size minimizes wall effects and accommodates conditions of relatively large sheath dimensions.

Chamber A includes a 15 cm diameter inductively coupled hf discharge, a 0.7 m x 1 m plasma flow chamber, a 20,000 1/s cryopump, and a roughing station. The vacuum characteristics are supported by micrometer leak valves, thermocouple and cold cathode ionization gauges, and a 20" diameter gate valve. In typical operations, the plasma flow and measurement capabilities are supported by four independent control grids, plasma neutralizers, and on-line diagnostics which include direct measurements of plasma density, temperature, plasma potential, mean-ion-mass, and density fluctuation power spectra. In addition, the diagnostics suite includes four channel wave analysis for determination of turbulence spectra, cross-correlation functions, and three-dimensional dispersion relations. The sensors are mounted on linear and rotary motion feedthroughs. This mounting permits mapping the plasma characteristics throughout the entire plasma flow volume.

The inductively coupled plasma source is particularly versatile. With no active electrode in contact with the plasma, there are added degrees of freedom in controlling the plasma source potential and its flow characteristics. The source is also free of the limitations typical of hot-filament type devices as well as oxide-coated cathode discharges. Gas constituents and pressures are never a problem. The source can strike and maintain plasma discharges from 10^{-6} to 200 millitorr. The system has been used for positive and negative ion plasma studies, including Ar^+, N^+_2, N^+, and SF^-_6. Scaled simulations of SF^-_6 mass-spectrometer parachute experiments were conducted in Chamber A. Using a scaled version of the 1-D flux cell, plasma ion and electron densities and electric fields were mapped within and upstream of the 1-D flux cell to determine the efficiency of negative ion conversion as a function of pressure and SF_6 injection rates.

Chamber B is an 8' x 15' (2.43 m x 4.57 m), LN_2-lined chamber equipped with roots blower and cyropumping. This chamber has the same plasma and neutral gas capabilities defined for the smaller system. Chamber B, however, has wider applications for large instrument tests and plasma simulation experiments requiring relatively large Debye lengths.

4.2 Specific Tasks

The goal of the 24-month effort was to demonstrate and validate the PIMS concept. We proposed to design and build the necessary sensor configuration and support electronics, and to implement chamber simulation tests over a pressure range equivalent to the 60-130 km domain and a mass range from approximately 16-125 amu. To accomplish these goals, we:

1. Designed, built, and tested the voltage pulsing circuitry and the electrometer circuitry with μs risetime characteristics. This effort included:

A. Detector-Surface Voltage Drivers with high slew rate op-amps capable of driving up to 100 uA. The circuit used a single debounced switch to change the voltage on 2 of the driver outputs with levels selected by adjustable potentiometers.

B. A Collector Current Monitor capable of recording uA currents at 1 Mhz bandwidth. This was the ultimate goal, but primary designs revolved around the PTA-100 Transimpedance Amplifier with a 200 Khz bandwidth for currents measured using the (10^{-5}) A/V gain scale. This provided a 5 μs response time for currents in the range of 1uA to 30uA. Faster risetime with increased sensitivity were accomplished with channeltron detection.

C. Testing - The circuits were tested to ensure the desired design characteristics. Surface voltage drivers were tested by attaching a scope probe to each surface (Aperture, Discriminator, Suppressor and Collector). The pulse risetimes were measured for the Suppresser and Discriminator surfaces. Collector tests were made by connecting a variable resistor from the collector to system ground. The variable resistor was sized to cover the complete sensitivity range and calibration procedures were recorded.

2. Implemented proof-of-concept validation tests for positive ions in the continuum regime.

A. Performed ion tests with Ne, Ar, and Kr providing mass selections 20.18, 39.94, and 83.7 amu, respectively. These tests were performed on each species individually to explore time of arrival vs mass characteristics. The chamber pressure was varied in seven steps, including 10^{-3}, $2(10^{-3})$, $5(10^{-3})$, 10^{-2}, $2(10^{-2})$, $5(10^{-2})$, and (10^{-1}) Torr for each of the gases.

B. Tests were repeated for mixes of Ne, Ar, and Kr, including mixtures of Ne/Ar and Ne/Kr. The relative concentrations of each gas were determined by the ionization potential of each element. Data were correlated with that collected in task item 2A. Pressure ranges included 10^{-3}, 10^{-2}, and 10^{-1} Torr for each of 2 gas mixes.

3. Implemented proof-of-concept validation tests for positive ions in the collisionless regime using channeltron detection.

A. Performed Ion tests with Ne, Ar and Kr providing mass selections 20.18, 39.94 and 83.7 amu, respectively. These tests were performed on each species individually to explore time of arrival vs mass characteristics. The chamber pressures were varied in a "survey" mode covering four pressure levels at $5(10^{-6})$, 10^{-5}, $5(10^{-5})$, and 10^{-4} Torr for each of 3 gases.

B. Tests were repeated for mixes of Ne, Ar and Kr and for gas mixtures of Ne/Ar and Ne/Kr. Data was correlated with that collected in task 3A covering the same pressure levels.

4. Revisited tasks 2 and 3 for negative ions using SF_6 with increasing levels of collisionality and ion detection searches focused on F^-(19 amu), SF^-_5 (127 amu), and SF^-_6 (146 amu).

4.3 Sensor Configurations and Chamber Test Results

Three sensor configurations were built and tested in order to develop an understanding for the impact of geometry on overall detection capabilities. Those sensors are shown in Figures 8 through 10. Purposes of each configuration were as follows:

1. Phase 1 geometry, shown in Figure 8, was a configuration adapted from an earlier PD[3] design, making it possible to develop an early empirical appreciation for grid spacing, suppressor voltage influences, collector plate efficiency, and ion optics.

2. Phase 2 geometry represented a modification to the sensor to mitigate side wall influences on ion optics and improve current collection/sensing capabilities.

3. Phase 3 geometry represented a flight prototype configuration that maximized optics and sensitivity, and included channeltron detection of ions passed through a "pinhole" aperture in the collector plate. This allowed "coarse" sensing capabilities through electrometer circuitry and pulse counting techniques for maximum sensitivity using the channeltron.

Figure 11 shows the Phase 3 sensor geometry installed for test in chamber A. Also seen in the figure are three movable Langmuir probes that allowed diagnostics of the plasma and its potential upstream from the PIMS aperture.

Before pulsed mode operations were executed it was necessary to execute swept mode diagnostics (quasi-dc operations) to study full details of ion optics and losses of ion beam currents to the aperture, suppressor and discriminator grids. It also made possible an understanding of PIMS performance characteristics relative to the conditions in the ambient plasma - particularly the ambient plasma density and plasma potential. An illustration of these results is presented in Figure 12. Test conditions in the illustration were in argon at a pressure of 3.0 $(10)^{-3}$ Torr, with the aperture, discriminator, suppressor, and collector voltages at $V_a = 5$, $V_d = 6$, $V_s = -2$, and $V_c = 3$ volts, respectively.

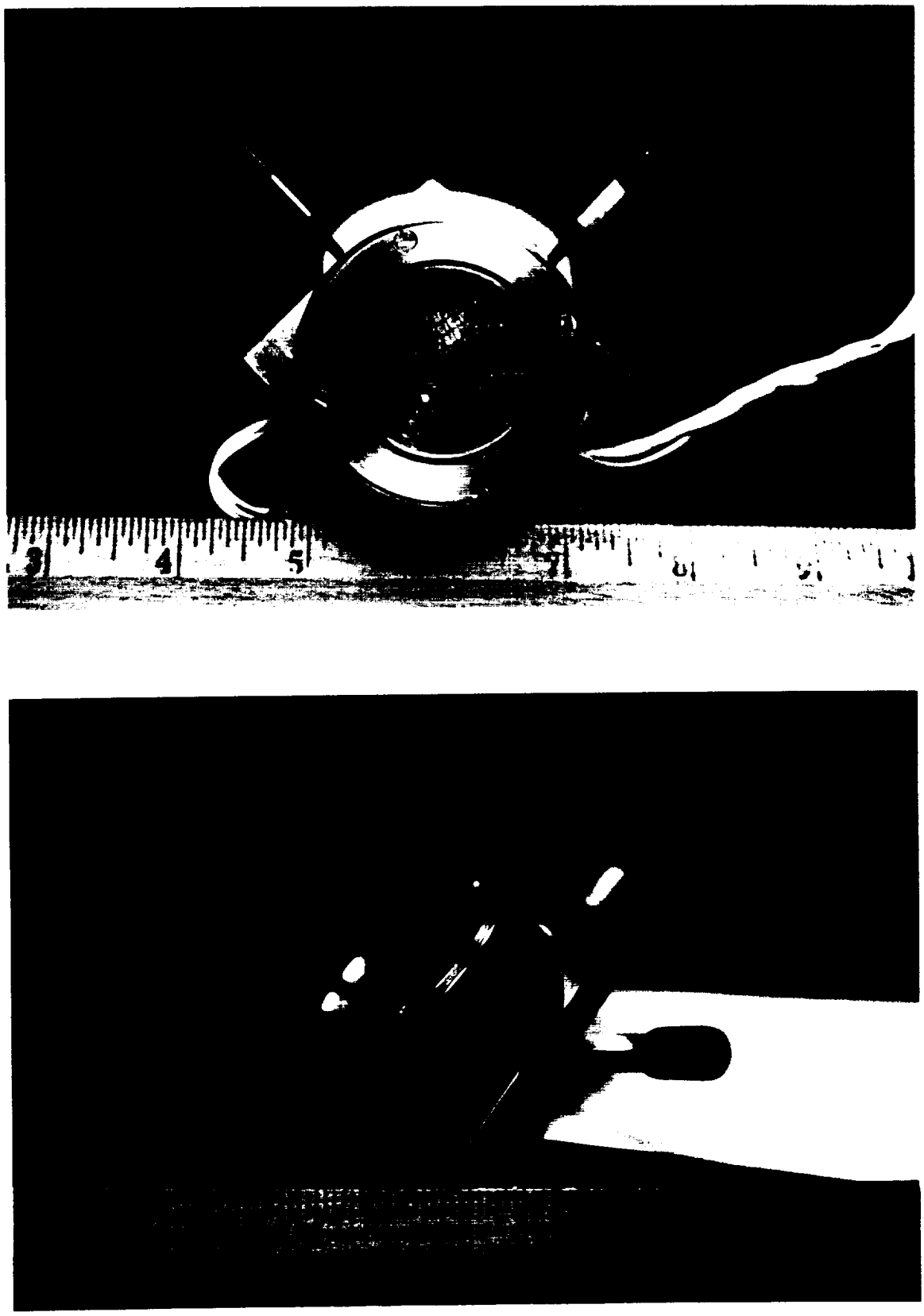

Figure 8. Phase 1 PIMS Geometry

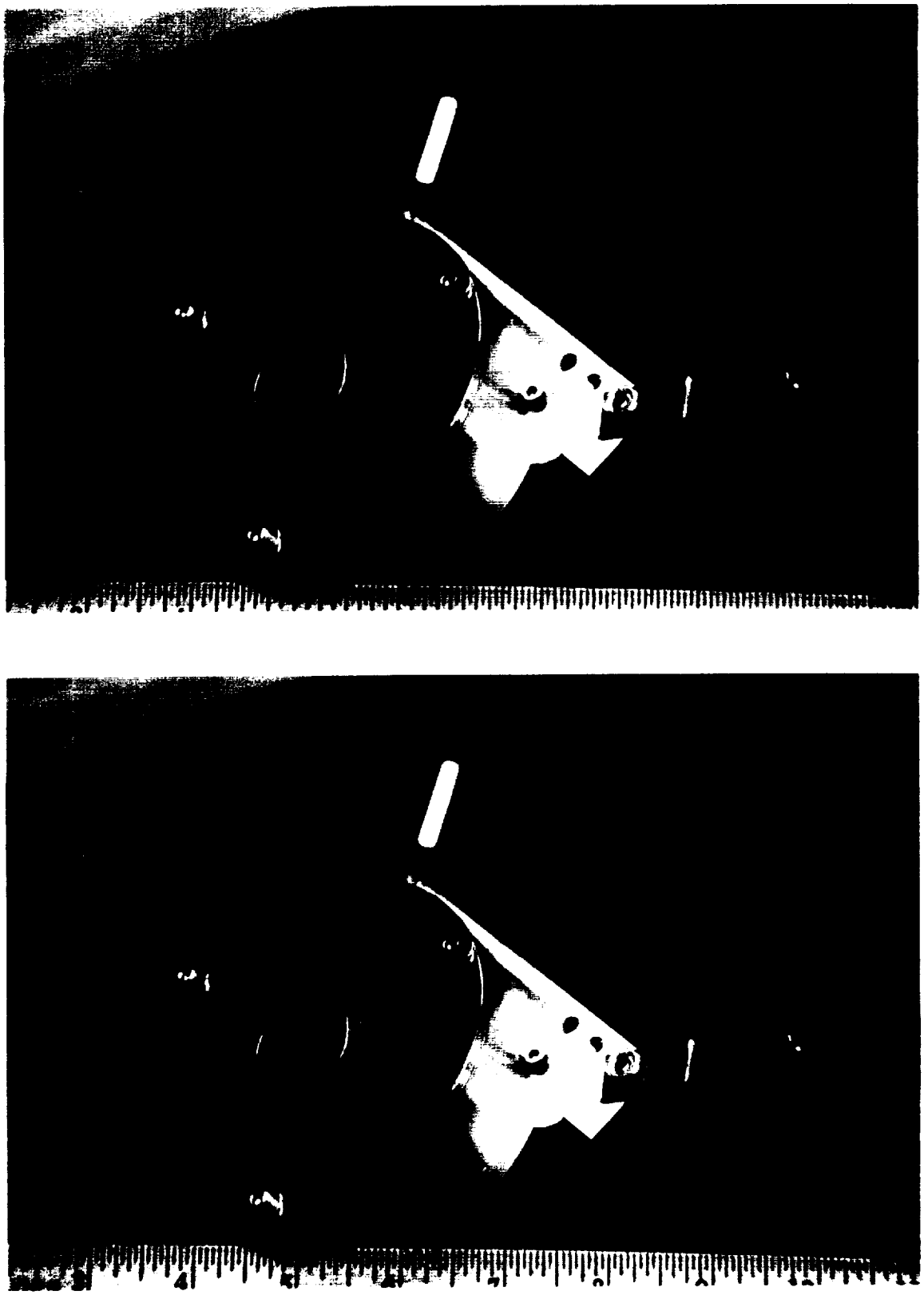

Figure 9. Phase 2 PIMS Sensor Geometry.

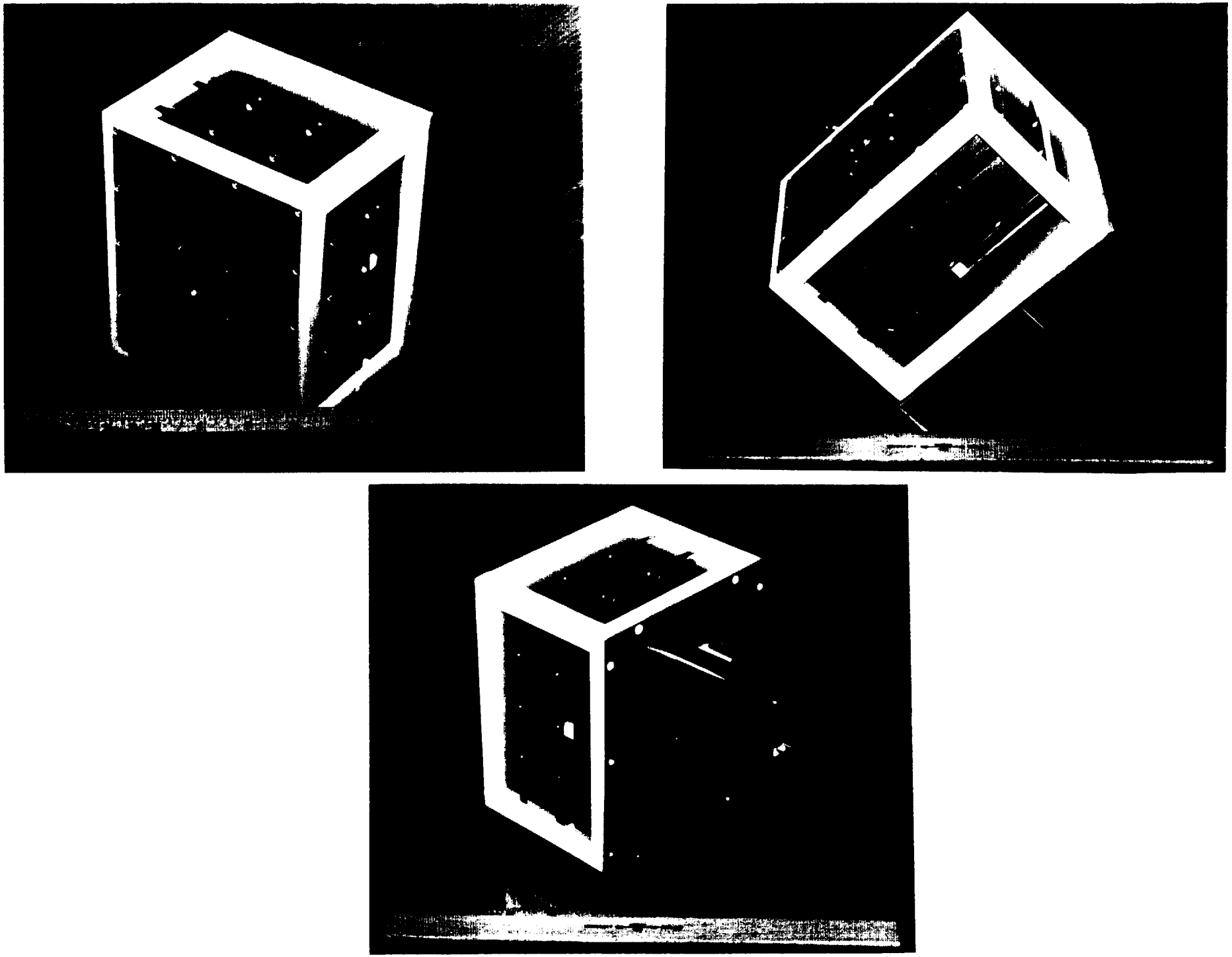

Figure 10. Phase 3 PIMS Sensor Geometry.

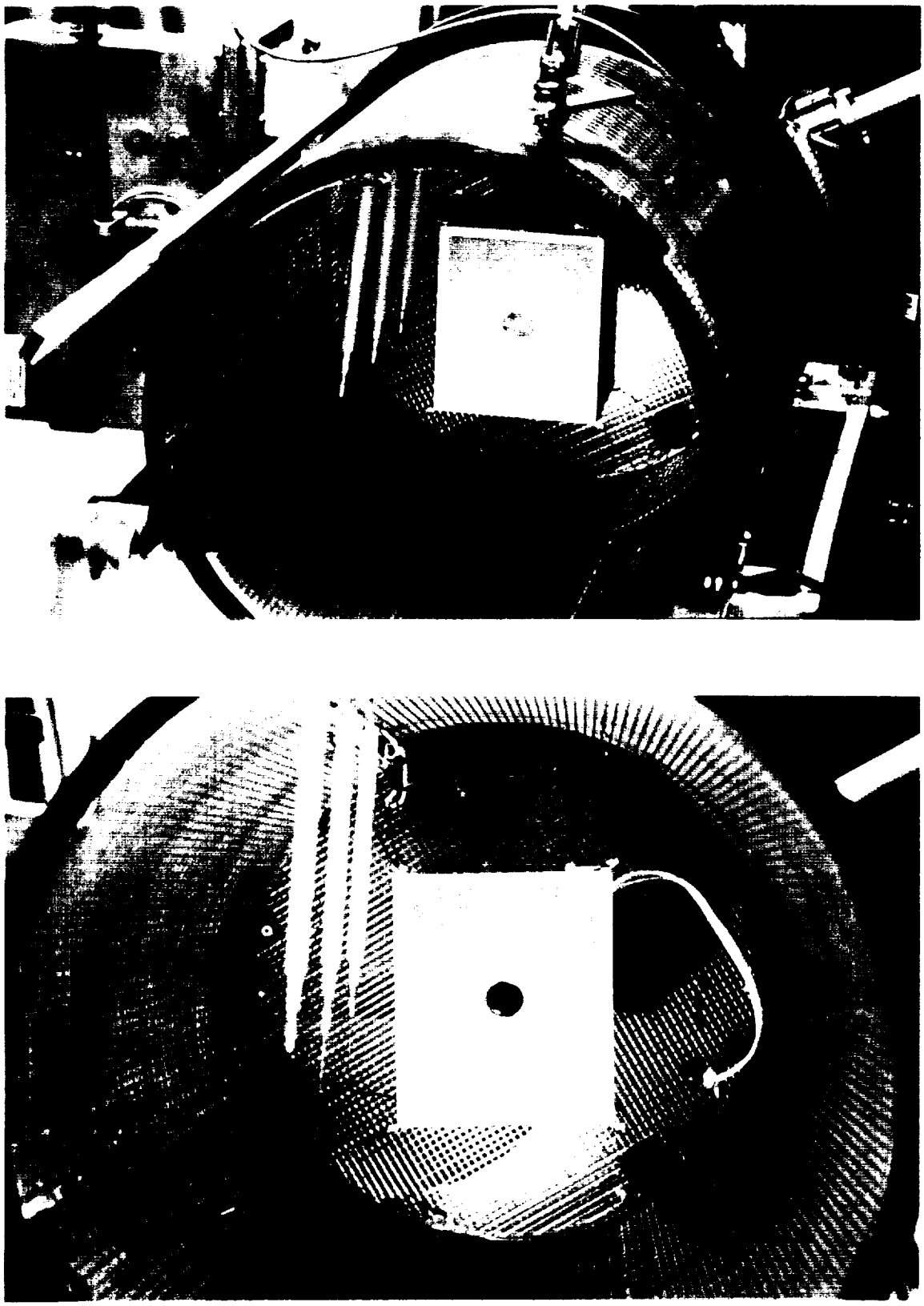

Figure 11. Phase 3 PIMS Sensor Configuration Under Test in Chamber A.

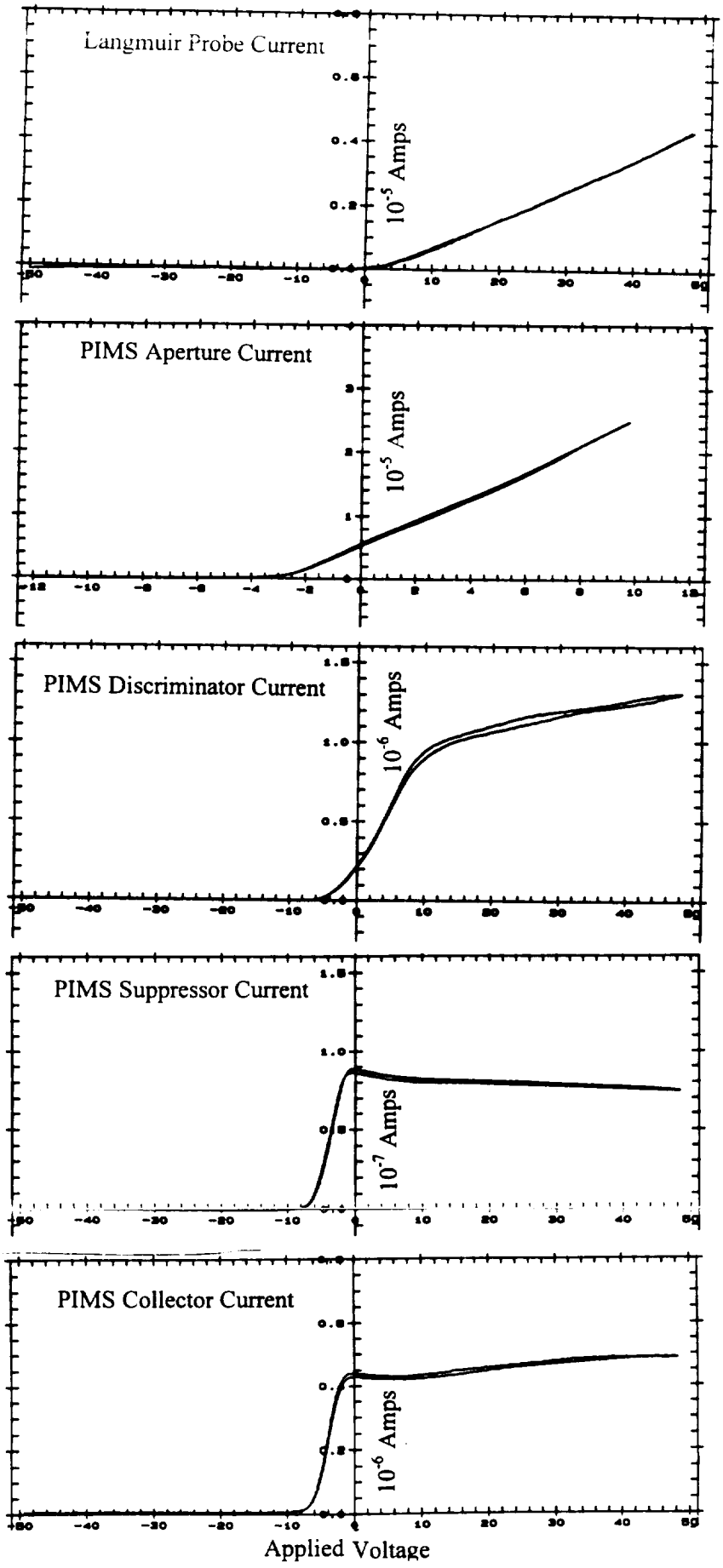

Figure 12. Swept Mode PIMS Operations.

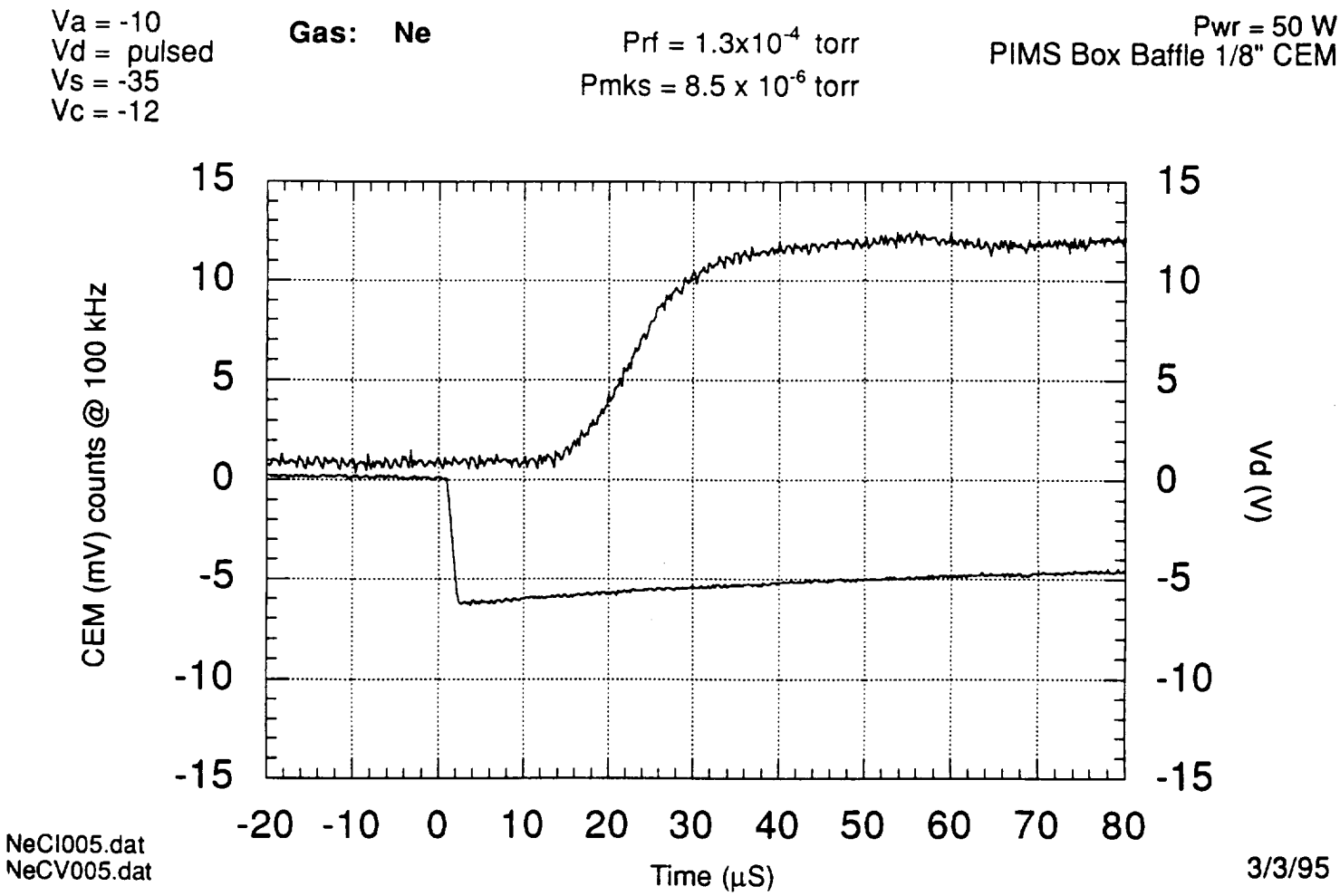

Figure 13. Pulsed Mode PIMS Operation in a Ne^+ Plasma at 1.2 (10^{-4}) Torr.

An illustration of successful pulsed-mode PIMS operation in a single species positive ion plasma environment is illustrated in Figure 13. This case was in neon at a pressure of $1.3(10)^{-4}$ Torr, with V_a = -10, V_s = -35, and V_c = -12 volts, respectively. Delay between the onset of the discriminator pulse and the arrival of the center of the Maxwellian ion "beam" is seen to be 20 μs. This is in good agreement with predictions for the Phase 3 sensor drift length (10 cm) and accelerating potential within the sensor itself (2 volts) coupled with a pre-aperture sheath acceleration at an estimated level of 8 volts (see Figure 3, collisionless-case for theoretical predictions). Test results like these were conducted for other species with similar success, but mixtures were not diagnosed because of channeltron failure in the closing weeks of the investigation. Conclusions relative to proof-of-concept then are limited only to single ion detection capabilities, but accumulated results indicate that multi-ion diagnostics should be achievable in cold ion distributions. "Hot' distributions tend to "smear" the temporal characteristics of the arriving ion pulse and complicate the unique identification of individual ion constituents. This is not a problem in near-Earth space plasma applications.

4.4. Lessons Learned

Parasitic effects of inter-electrode capacitance tended to be a constraint on temporal resolution and current sensitivities. Future designs (in both the sensor and the electronics) can mitigate this problem and bring the specifications to the required level for mesospheric and lower-thermospheric applications. Future designs must also incorporate "smart" aperture potentials - that is, electronic systems that provide real-time monitoring of the ambient plasma potential and an automatic re-setting of aperture potentials to guarantee ion collection without inducing large accelerating potentials in the aperture pre-sheath. This is do-able with interspersed operations of the aperture plate as a pulsed Langmuir probe itself and then as a passive aperture plate for "standard" PIMS operations. And finally, ideal operations should include simultaneous electrometer and channeltron detection to encompass the broadest possible range of sensitivities. For applications over the 60-130 km regime, this would require differential pumping to guarantee channetron performance and life.

REFERENCES

1. Kennel, C. et al., "Executive Summary - Report of the Mission Integration, Divisional Science Panel (Space Physics Strategy Implementation Study)," NASA Headquarters Report (Pre-print, November 28, 1990).

2. Szuszczewicz, E.P. et al., "The NASA Program in Ionospheric-Thermospheric-Mesospheric Physics for 1995-2010: Final Report of the ITM Panel," NASA Headquarters Report (November 1990).

3. Reid, G.C., :"Electrical structure of the middle atmosphere," The Earth's Electrical Environment, pp. 183-194, eds. E.P. Kridler and R.G. Roble, National Academy Press, Washington, D.C. (1986).

4. Swider, W., Rad. Sci 23, 389 (1988).

5. Brasseur, G., and P. DeBaets, J. Geophys. Res. 91, 4025 (1986).

6. Szuszczewicz, E.P., J. Geophys. Res. 79, 1083 (1974)

7. Meyerott, R.E. et al., J. Geophys. Res. 85, 1273 (1980).

8. Szuszczewicz, E.P. and J.C. Holmes, J. Appl. Phys. 46, 5134 (1975).

9. Mitchell, J.D., "Rocket probe techniques for measuring bulk ion properties," pp. 155-172 in Middle Atmosphere Programs 19, ed. R.A. Goldberg, published by ICSU/SCOSTEP (1986).

10. Hale, L.C. and C.L. Croskey, Nature 278, 239 (1979).

11. Maynard, N.C. et al., Geophys. Res. Lett. 8, 923 (1981).

12. Kelley, M.C. et al., Geophys. Res. Lett.10, 733 (1983).

13. Szuszczewicz, E.P. and J.C. Holmes, Rev. Sci. Instr. 46, 592 (1975).

14. Szuszczewicz, E.P. and J.C. Holmes, AIAA 76-393, 9th Fluid Dynamics Conference (1976).

15. Shen, J.S. et al., J. Geophys. Res. 18, 5517 (1976).

16. Wilkinson, P. et al., Geophys. Res. Lett. (1991, in press).

17. Mathews, J.D. and F.S. Bekeny, J. Geophys. Res. 84, 2743 (1979).

18. Mathews, J.D., "Some aspects of metallic ion chemistry and dynamics in the mesosphere and thermosphere," in Middle Atmosphere Programs, MAP Vol. 25, 228 (1988).

19. Bills, R.S. and C.S. Gardner, Geophys. Res. Lett. 17, 143 (1990).

20. Franke, S.J. et al., Geophys. Res. Lett. 17, 69 (1990).

21. Hanson, D. et al., Sp. Sci. Instr. 5, 1503 (1981).

22. Holmes, J.C. and E.P. Szuszczewicz, Rev. Sci. Instr. 46, 592 (1975).

23. Wehner, G. and G. Medicus, J. Appl. Phys. 23, 1035 (1952).

24. Hiroa, K. and K. Oyama, J. Geomagn. Geoelectr. 24, 415 (1972).

25. Gains, G.L., in Scientific Foundations of Vacuum Techniques, 2nd Ed., ed S. Dushman and J.M. Lafferty (Wiley, New York, 1966), p. 376; E.W. McDaniel, Collision Phenomena in Ionized Gases, (Wiley, New York, 1964) Chap. 13.

26. Winters, H.F. and P. Sigmund, J. Appl. Phys. 45, 4760 (1974).

27. Singh, M. and E.P. Szuszczewicz, J. Geophys. Res. 89, 2313 (1984).

28. Szuszczewicz, E.P. et al., J. Geophys. Res. 87, 1565 (1982).